



UPPSALA  
UNIVERSITET

Serienummer

Examensarbete 30 hp

Januari 2023

# Hanging load mock-up for experimental setup to test flight system stability

A Master's Thesis in Electrical Engineering

---

Anthony Gundstedt



UPPSALA  
UNIVERSITET

## Hanging load mock-up for experimental setup to test flight system stability

---

Anthony Gundstedt

### Abstract

Can we reduce disturbance, swing, and errors by delegating some of the tasks to a subsystem on the tool hanging from a drone to gain precision and dependability? This project covers developing and implementing a user-controlled prototype with an automatic control system and gripper for functionality and controlled movement in 5 DOF.

AirForestry is developing a new way of working in the forestry business to provide a greener and healthier solution for the soil and the environment. The forestry industry emits approximately one million tons of CO<sub>2</sub> per year from heavy diesel-fueled vehicles. With a renewable energy battery-powered drone of a diameter of 6.2 m and a hanging harvesting tool, they can significantly improve the environmental impact of forestry. The harvesting tool has an automatic control system and is user controlled to perform the thinning and cutting of trees.

The main focus is to use IMU sensor data to produce accurate angle estimation to control the stability of a scaled prototype and to implement physical restrictions to make it able to be attached safely and tested on a drone but not limit the controlled mobility of the prototype with a system independent of the control system of the drone itself. The user can control the attitude and elevation and receive real-time sensor data wireless during operation. With the intended spacing of the attachment points on the drone, it can prevent unwanted swing from a push or displaced drop. It uses the accelerometer on the IMU sensor to calculate the angle of roll and pitch, although the accelerometer is sensitive to vibrations and rotations. The control system has a fast response and rise time, but it experiences noise and oscillations. Sensor fusion of the accelerometer and gyroscope in a complementary filter can be implemented to increase the accuracy of the angle estimations and decrease the noise, which will be reflected in the speed of the servos and thereby improve the stability and mobility of the system.

**Teknisk-naturvetenskapliga fakulteten**

**Uppsala universitet, Utgivningsort Uppsala**

Handledare: August Tynong Ämnesgranskare: Kjell Staffas

Examinator: Mikael Bergkvist

# Populärvetenskaplig sammanfattning

Föreställ dig att bli av med 20% av det du äger bara för att kunna förvalta de resterande 80% i din ägo. Så är det idag för många skogsägare som tvingas framföra tunga dieseldrivna skogsmaskiner för att sköta om sitt skogsbruk. Detta vill start-up-företaget AirForestry ändra på. Ett högteknologiskt företag som utvecklar drönare med 6.2 m i diameter och tillhörande skövlingsverktyg för att från luften, helt automatiserat och eldrivet, skövla skogs på ett hållbart sätt. För att detta verktyget ska kunna kvista och kapa träd samt transportera stammen krävs kontrollerbarhet, pålitlighet och precision.

Detta projektet består av att utveckla en styrbar batteridrivnen prototyp av verktyget som, istället för att hantera träd, ska kunna plocka upp och släppa av upp till 5 kg last samt trådlöst kunna ta emot och sända ut värdefull data. Så sköter drönaren flygningen. Drönaren är avsedd för att vara 1.2 m. Verktyget använder sig av sensorer, dels för att kunna vara parallell mot marken under hela flygningen, men även för att användaren ska kunna kontrollera verktyget och ha kunskap om distansen till marken eller till en trädkrona. Av de tilldelade uppgifterna som utvecklades var möjligheten att kontrollera prototypens rörelser i sidled, höjdläge och lutning framåt och sidled. En mjukvarulösning för att motverka en svängning utvecklades ifall en kastvind eller en plötslig rörelse från drönaren skulle initiera en svängning. Orsaken till detta är för att försöka minska störningar, fel och svängningar medans man ökar precision och pålitlighet hos det hängande verktyget.

Resultatet av arbetet är sex mekaniska komponenter som bland annat vinstyck och sensor-hållare. Med de elektriska komponenterna, ett regelsystem och programmerad mjukvara, kan detta verktyget styras av användaren med smarta restriktioner och noggranna mätvärden. Anti-swing funktionen presenteras i tre versioner där en implementeras som effektivt hämmar svängningar vid det tilltänkta avståndet av fästpunkterna.

# Contents

<b>1</b>	<b>Introduction</b>	<b>9</b>
1.1	Background . . . . .	9
1.2	Problem statement . . . . .	9
1.3	Requirements . . . . .	9
1.4	Goals . . . . .	10
1.5	Reporting & follow-up . . . . .	10
<b>2</b>	<b>Theory</b>	<b>12</b>
2.1	S.BUS . . . . .	12
2.2	$I^2C$ . . . . .	12
2.3	Over-the-Air programming . . . . .	13
2.4	Closed-loop control system . . . . .	13
2.5	PID-controller . . . . .	14
2.6	Drone functionality . . . . .	15
2.7	Anti-swing . . . . .	16
2.7.1	Playground swing set . . . . .	16
2.7.2	Lateral movement . . . . .	16
2.8	Designing theory . . . . .	17
<b>3</b>	<b>Method</b>	<b>18</b>
3.1	Overview of the system . . . . .	18
3.2	Hardware and components . . . . .	18
3.2.1	CAD-models . . . . .	19
3.2.2	Servo motors . . . . .	19
3.3	Sensors . . . . .	19
3.3.1	IMU . . . . .	19
3.3.2	Altimeter . . . . .	20
3.3.3	Ultrasonic sensor . . . . .	20
3.4	Configuration and Filtering . . . . .	20
3.5	Software and development tools . . . . .	21
3.5.1	Telnet . . . . .	21
3.5.2	Visual Studio Code and PlatformIO . . . . .	21
3.5.3	Fusion 360 . . . . .	21
3.6	Implementation . . . . .	22
3.6.1	Design and Construction . . . . .	22
3.6.2	Assembly and Configuration . . . . .	23

3.6.3	Anti-Swing and Optimization . . . . .	24
3.6.4	Mixer matrix . . . . .	26
3.6.5	Get attitude from x,y,z-components . . . . .	26
3.6.6	Attachment points to the drone . . . . .	27
3.7	Process flow diagram of the PID controller . . . . .	27
3.8	Hardware implementation . . . . .	29
3.9	Pinout . . . . .	30
3.10	Testing . . . . .	31
3.10.1	Calibration . . . . .	31
3.10.2	Mobility and Functionality . . . . .	32
3.10.3	Stability . . . . .	32
3.10.4	Anti-swing . . . . .	32
3.10.5	Counteract yawing . . . . .	34
3.10.6	Attached to the drone . . . . .	34
<b>4</b>	<b>Results</b>	<b>35</b>
4.1	Design and Construction . . . . .	35
4.2	Tests . . . . .	35
4.2.1	Passive leveling . . . . .	35
4.2.2	Elevation . . . . .	36
4.2.3	Mobility . . . . .	39
4.2.4	Functionality . . . . .	40
4.2.5	Anti-swing . . . . .	43
4.2.6	Accelerometer testing . . . . .	47
4.2.7	Attachment to the drone . . . . .	49
<b>5</b>	<b>Discussion and further work</b>	<b>50</b>
5.1	Analysis of the method . . . . .	50
5.2	Analysis of the results . . . . .	51
5.2.1	Anti-swing . . . . .	52
5.2.2	Test with narrow attachment . . . . .	52
5.2.3	Narrow anti-swing . . . . .	53
5.2.4	Accelerometer . . . . .	53
<b>6</b>	<b>Conclusion</b>	<b>55</b>
6.1	Requirements . . . . .	55
6.2	Goals . . . . .	55
6.3	Problem statement . . . . .	55

6.4	Further work . . . . .	56
6.4.1	Hardware & components . . . . .	56
6.4.2	Software and the utilization of sensor data . . . . .	56

## List of Figures

1	Electrical connection in $I^2C$ [1] . . . . .	13
2	Bit by bit call writes from master to slave with address 1100100[1] . . . . .	13
3	Closed-loop control system[2] . . . . .	14
4	Playground swing . . . . .	16
5	Reduction of swing with lateral variation[3] . . . . .	17
6	The complete prototype . . . . .	18
7	Triangle plate for servo and box . . . . .	22
8	Box for electronics . . . . .	23
9	Winches for the servos . . . . .	24
10	Case for ultrasonic sensor . . . . .	25
11	Gripper to lift object with . . . . .	25
12	Wire holder for the winches with the wire hole red-marked . . . . .	26
13	Automatic control system for roll . . . . .	28
14	Circuit diagram with all components . . . . .	30
15	Espressif ESP32-DevKitC pinout[4] . . . . .	31
16	Stability test from horizontal without external influence . . . . .	36
17	Height test with target elevation and distance to ground . . . . .	37
18	Elevation test with narrow attachment . . . . .	38
19	Target angles(tRoll, tPitch) and measured roll and pitch . . . . .	39
20	Grip and elevation test . . . . .	40
21	Stability from non-horizontal and during elevated . . . . .	41
22	Servos during non-horizontal stability test . . . . .	42
23	Functionality test of roll, pitch & elevation with narrow attachment . . . . .	43
24	Swing without servos . . . . .	44
25	Anti-swing with servos and three external forces applied . . . . .	44
26	Swing with servos powered off from 1m . . . . .	45
27	Roll and pitch during anti-swing . . . . .	46
28	Servo writes during anti-swing . . . . .	47
29	Accelerometer during anti-swing . . . . .	47
30	Accelerometer at stand still . . . . .	48
31	Rotational movement around the z-axis . . . . .	48

## List of Abbreviations

$I^2C$	Inter-Integrated Circuit
$V_{dd}$	Positive supply voltage
CAD	Computer-Aided Design
DOF	Degree of freedom
FIFO	First-In-First-Out
GPIO	General Purpose Input/Output
IMU	Inertial Measurement Unit
MCU	Microcontroller Unit
MEDEVAC	Medical evacuation
OTA	Over-The-Air
PID	Proportional-Integral-Derivative
PWM	Pulse-Width Modulation
RC	Radio-Controlled
RPM	Revolutions Per Minute
RX	Receive
SCL	Serial Clock
SDA	Serial Data
SDK	Software Development Kit
SPI	Serial Peripheral Interface
SSH	Secure Shell
TX	Transmit



# 1 Introduction

This section will provide information about the background of the company and this project. It will also cover the project's problem statement, requirements and goals.

## 1.1 Background

AirForestry is a start-up that develops drones with a diameter of 6.2 meters, equipped with a hanging harvesting tool to thin and cut down trees in the forest to make the forestry industry greener and more sustainable. It requires the tool to be able to move in specific directions and perform the tasks it is supposed to do. To test the concept of flying a drone with variable length, weight and a control system. A down-scaled prototype of the tool and the drone is being developed and manufactured. The project will help test the whole system's theoretical model with lower costs and risks to help discover unpredictable behavior and validate assumptions.

Publications have been written about drones with hanging loads with variable length pendulums[5], swing-free trajectories[6] on cranes, helicopters[7] and drones[8]. Documentation regarding wireless data transmission to user[9], filtering and stabilization. These implementations are often done with one or several vehicles controlling the load stability, position and orientation. The object the vehicle carries is often not the critical part and many times it is just defined as a body of mass.

This project combines all these different areas and relies on the load, or tool in this case, to do all these things by itself. Furthermore, it will also be able to pick up more load with a gripper and drop it on command by the user.

## 1.2 Problem statement

Is it possible to reduce disturbance, swing and errors by delegating some tasks to a subsystem on the tool to gain precision and dependability? How will such a tool affect drone movement and flight control?

## 1.3 Requirements

- The total amount of load has a total of 5 kg, including the tool itself.

- Manufacture a user-controlled wireless physical battery-powered scaled prototype that can be attached to a smaller version of the 6.2-meter drone to pick up and drop off a load.
- Have three attachment points to the drone with winches to create variable-length wires.

## 1.4 Goals

- The system should be able to filter the input data from the sensors to produce accurate estimations.
- The tool should be auto-stabilized with an automatic control system and be able to move manually in 5 DOF with an RC transceiver. These are ascending, descending, sideways and forward movement, pitch and roll, corresponding to acceleration in the x,y and z-axis and rotating along the x, y-axis.
- Wireless data transmission and data analysis to the driver during operation.
- Connect the tool to a drone and test the system during flight.

Moreover, if time allows:

- The prototype should be able to mitigate unwanted swings from a 1-meter horizontal push on the tool, which can be resembled an unwanted swing induced by the drone or external forces like wind.
- The tools should have a way to counteract and prevent yawing, rotation around the z-axis, of 360° in both clockwise and counterclockwise directions—the 6th DOF.

## 1.5 Reporting & follow-up

The project will be documented in this project plan, Gantt-chart, the Air-Forestry Google drive and as a report published on DiVA. The project will then be presented and critically reviewed at Uppsala University in the presence of relevant individuals, such as the Subject reviewer, Supervisor, Coordinator and Examiner. Except for the initial meeting with the Subject

reviewer, contact will occur at hand in of revised project plan, halfway done with the report and when it is time for the approval to be present but the contact is not limited to these occasions and the student is welcome to contact the subject reviewer in a matter of need. The communication between the supervisor and the student is continuous and the time is approximately 5 hours per month, but the student can also ask other company employees for assistance.

## 2 Theory

This section covers the theory and working principles that are required to understand and complete the project.

### 2.1 S.BUS

S.BUS or Serial BUS is an option when controlling servo motors more accurately using serial data. Servos typically use PWM to manipulate the speed of the motors, but then one signal wire is required per servo motor. Digital S.bus servos accept 11 bits signals, including an even parity bit, two stop bits, and 8 data bits and have a baud rate of 100000. The protocol is 22 bytes long and can manage 16 individual servos using only one wire for transmission(TX) and one receives data from the system with one wire(RX).

### 2.2 $I^2C$

$I^2C$ , short for Inter-Integrated circuit, is a synchronous serial multi-master bus used to connect various units and sensors in, for example, smartphones, embedded systems and other electronic devices. Four wires are needed to establish the protocol, including Voltage in(Vdd), ground, SDA and SCL. SDA is the serial data line that carries the data signal and SCL is the serial clock line. The Voltage is normally either 5 V or 3.3 V. The protocol is often used between microcontrollers and sensors. These are traditionally called Master and Slave and this protocol can handle multiple Masters and multiple slaves. Figure 1 is an example of the electrical connection between one Master and three slaves, all connected to SDA, SCL and VDD. Every unit in the protocol has a unique address called when sending or receiving data. The protocol start with SDA pulled low, then a 7-bit address, followed by a read/write bit. Here the caller waits for the slave to acknowledge by pulling low and the caller continues with 8-bit data and then awaits another ack bit. More data bytes can also be sent with the same call. This procedure is also illustrated in figure 2.

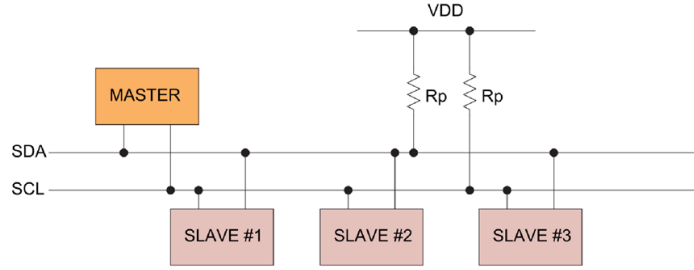


**Figure 1:** Electrical connection in  $I^2C$ [1]

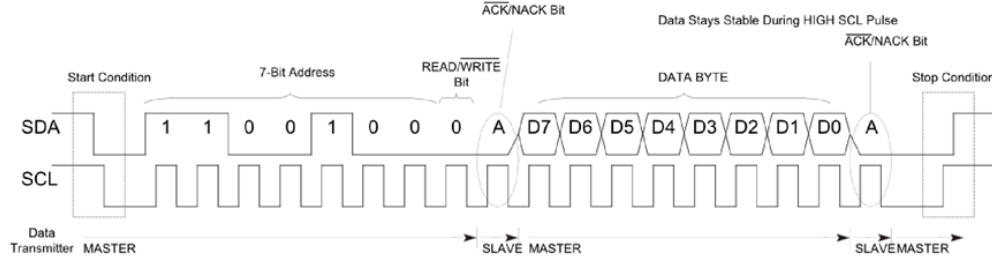


**Figure 2:** Bit by bit call writes from master to slave with address 1100100[1]

## 2.3 Over-the-Air programming

The OTA update is a method to configure settings and distribute new software to units like a microcontroller, mobile phones, electric cars and embedded units. It is used to update the software in the microcontroller with WiFi when a computer-to-microcontroller cabled connection is impossible. The OTA method needs to be initialized before usage since it is an active function not implemented by default.

## 2.4 Closed-loop control system

A closed-loop control system is an electrical and mechanical process that regulates a system to automatically maintain a desired set point or state without human interaction. It uses a feedback system or sensors to inform how far the output is from the set point. The system consists of blocks called controller, actuator, process, and sensor and can be seen in Figure 3 below.

The controller is a PID controller, the actuator is the servos and the process is the prototype.

On the far left is the set point or reference input, subtracted by the feedback signal, becoming the error. The disturbance is added after the actuator in the figure, which is a simplification of noise and disturbance from the input signal, actuator noise and process disturbance primarily due to the winch wires not being completely stiff.

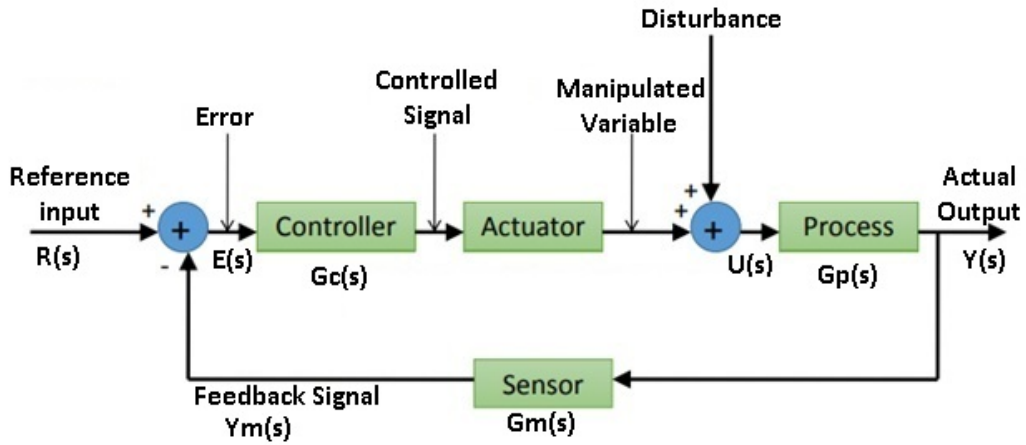


Figure 3: Closed-loop control system[2]

The equation of this system in the Laplace domain is determined by

$$\begin{aligned}
 Y(s) &= G_p(s)G_c(s)E(s) \\
 Y(s) &= G_p(s)G_c(s)[R(s) - Y_m(s)] \\
 Y(s) &= G_p(s)G_c(s)[R(s) - G_m(s)Y(s)] \\
 Y(s) &= \frac{G_p(s)G_c(s)}{1 + G_p(s)G_c(s)G_m(s)}R(s)
 \end{aligned} \tag{1}$$

The goal of the system expressed through this equation is  $\frac{Output}{Input} = \frac{Y(s)}{R(s)} \rightarrow 1$

## 2.5 PID-controller

Proportional-integral-derivative-controller is used automatic control system. With the feedback loop, an estimated error between the current and reference

values can be used to control the system sufficiently. The mathematical equation for the controller in the time domain is presented in Equation 2[10], where  $r$  is the reference signal, and  $y$  is the controlled output signal.  $K$ ,  $T_i$  and  $T_d$  are the design parameters to be tuned specifically for each application. A simplified version of the equation expressed in terms of error looks like Equation 3. This is also how the design parameters will be treated during this project.

$$u(t) = K \left( r(t) - y(t) + \frac{1}{T_i} \int_0^t r(\tau) - y(\tau) d\tau + T_d \frac{d(r(t) - y(t))}{dt} \right) \quad (2)$$

$$u(t) = K_p e(t) + K_i \int_0^t e(\tau) d\tau + K_d \frac{d(e(t))}{dt} \quad (3)$$

The  $P$  term is proportional to the difference between the set point and the measured process value, which is the error. The  $K_p$  is responsible for how much the error should be corrected at any given time and a high  $K_p$  will result in a faster rise time. The  $I$  term takes the integral of current and past errors. Large values of  $K_i$  can lead to overshoot and oscillations. If the  $I$  term depends on past errors, the derivative term depends on future errors. In other words, the error rate changes, which will significantly impact when the reference signal is changed. The  $D$  term is often seen as the opposite of the  $I$  term and reduces overshoot. It can not bring the magnitude of the error to zero but its own, but with the  $P$  and  $I$  term, it can easily regulate many different systems.

## 2.6 Drone functionality

The drone is a hexacopter with angled propellers relative to the ground. A drone can move in 6 DOF, in x,y,z and rotation around x,y,z. The rotation is named roll, pitch and yaw, respectively, with the x-axis defined as forward. Half of the propellers rotate clockwise, and the other rotates counterclockwise to prevent unintentional yaw. Since it is fast, has a lot of lift force and is unpredictable from the prototype point of view, this needs to be accounted for. The size of the drone is 1.2 m in diameter, which is a scaled prototype of the full-size drone.

## 2.7 Anti-swing

Several things, like wind and drone movement, can cause swing. Swing is also highly dependent on how far the attachment points on the drone are from the center of the drone and how far the prototype is from the drone, in other words, how long the pendulum is. This project will focus on two theories of how to mitigate it.

### 2.7.1 Playground swing set

As one may remember from their younger years on the playground, when using the swing, is that you can not just stay still and maintain the same angular velocity on the swing if you do not have a friend pushing you. Instead, you had to accumulate that force of your own. That is done by leaning your upper body backward in position A in figure 4 and gradually moving your upper body forward until the endpoint in position E. In other words, the center of mass is positioned behind the pendulum and the body performs a positive pitch angle relative the direction of velocity. The same theory is used in reverse to counteract unwanted swing and applies a negative pitch angle relative to the velocity.

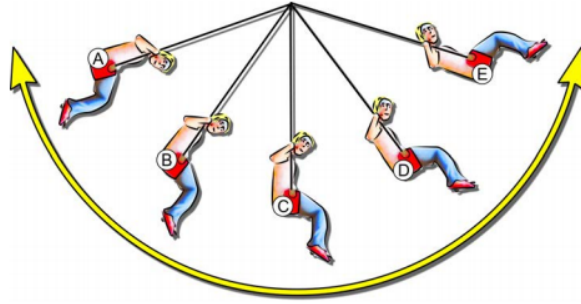


Figure 4: Playground swing

### 2.7.2 Lateral movement

In the paper "Suspended load swing stabilization" [3], they write about hoisting causalities into a MEDEVAC helicopter. They focus on automatic stabilization to reduce the personnel and time needed in a rescue. They refer to prior research by A. Kavanaugh and T. Moe[11] where they attempt to



widen the displacement angle of the object, which is the exact opposite of what is desired in MEDEVAC. The approach attempted in that research was letting out the rope in the middle and pulling it up in the end to lessen the displacement angle. It is also suggested to use two hoist ramp rates, slower right before and faster right after the mass reaches its maximum displacement angle. The paper concluded that this method can eliminate the need of a crew chief to take hold off the cable, lean out of the helicopter and stabilize the swing, thus increase the safety of medical and helicopter personnel.

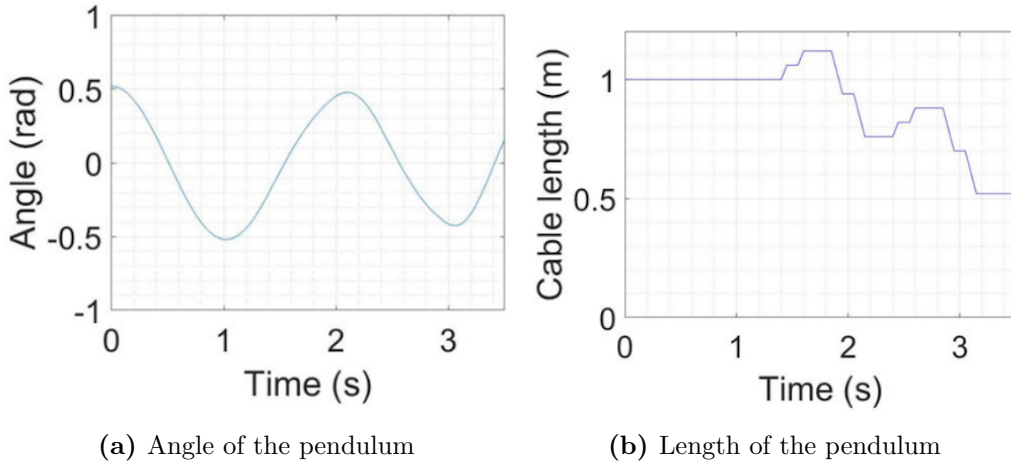


**Figure 5:** Reduction of swing with lateral variation[3]

## 2.8 Designing theory

The servos are evenly distributed around the edges of the prototype with  $120^\circ$  from each other, with a winch attached to each servo to provide space for the fishing line. It has a submerged box in the middle to lower the center of mass, which provides more control and prevents the prototype from falling over. The center of the box has an enclosure for the battery to keep it in place and keep the mass as centered as possible and away from the other components. On each side of the battery, there is space for the rest of the components except for the altimeter and IMU, which will be on top of the triangle-shaped plate. The gripper and the ultrasonic sensor are situated underneath the center box. The winches also have a wire holder to keep them from falling off the winch while flying or high-angled intentional or unintentional pitch and roll movements.

### 3 Method

This section starts with listing the hardware components and the software tool used, followed by the design of the non-electronic parts and implementation of the system, as well as a description of certain parts of the system, ending with an overview of the tests that will be made and displayed in the results section.

#### 3.1 Overview of the system

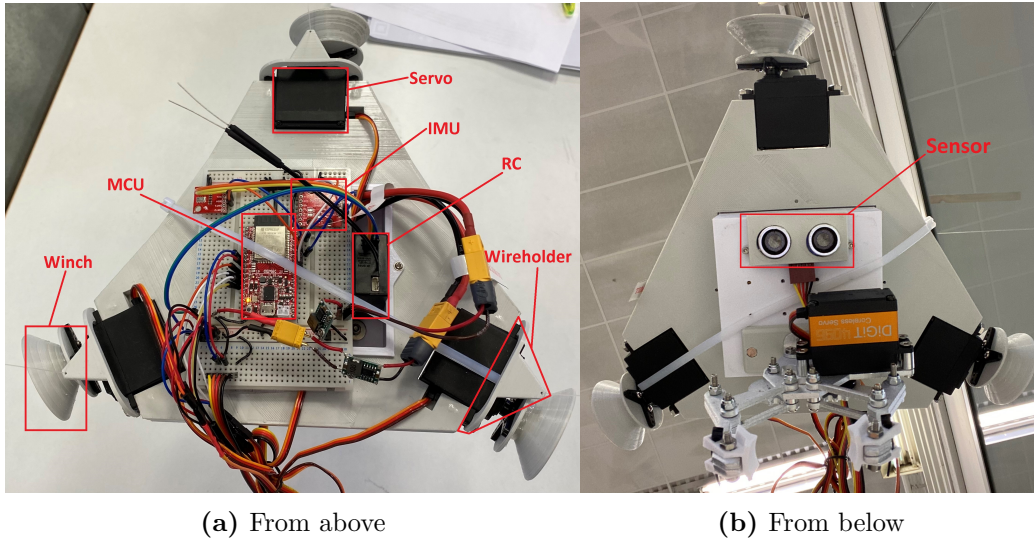


**Figure 6:** The complete prototype

#### 3.2 Hardware and components

The hardware that will be used in this project will be the microcontroller ESP32, continuous servo motors, inertial measurement unit (IMU), step-down DC/DC converters (Buck-converters), rechargeable 2S 7.4V battery, the radio receiver FrSKY archer R10 Pro, RC transceiver, altimeter, ultrasonic sensor, a regular servo for the gripper and nylon fishing line.

### 3.2.1 CAD-models

The non-electric parts of the prototype were designed in Fusion360 and ended up being seven individual designs used in the current version of the tool. The parts include a triangular plate, a box, winches, an ultrasonic sensor holder, a wire holder, a gripper mount, and a gripper attachment.

### 3.2.2 Servo motors

The prototype uses four servos: three are continuous and one is positional. The continuous servos are used for the winches to control the whole unit and the positional servo is for the gripper. All the servos have plastic gears which makes them fairly light. The speed without load is 60 RPM, peak stall torque of 6 kg · cm, and stall current of 1100 mA at 6V but can range between 4.8 – 6 V. The pulse width range is 700 – 2300  $\mu$ s with a stop position at 1500  $\mu$ s.[12] The positional servo has the same specifications only difference is that it gives a position rather than a specific velocity.

## 3.3 Sensors

Sensors are used in different ways to measure orientation, attitude, height and distance to the ground. The sensor measurements are then used in the closed-loop automatic control system to stabilize, roll, pitch and elevate the prototype.

### 3.3.1 IMU

The IMU is a sensor that measures acceleration, rotation and location with a built-in accelerometer, gyroscope and magnetometer. However, it can also measure temperature and has programmable interrupt sensors. It can measure up to 16 g linear acceleration, 16 Gauss magnetic and 2000 DPS, but it can also be scaled down to increase precision. Every measurement is in three dimensions which in other defined measurements in 9 DOF and can use both  $I^2C$ , in standard mode(100 kHz) and fast mode(400 kHz), and SPI(10 MHz) serial interfaces for communication with the microcontroller. In addition, this sensor will provide information about how the prototype is oriented.

### 3.3.2 Altimeter

This sensor measures pressure which it can convert to altitude using a standardized equation with an offset value and has a resolution down to 30 cm. It uses  $I^2C$  with clock frequency up to 400 kHz, has a data acquisition rate from 1 second up to 9 hours and can store data for up to 12 days using FIFO, first in, first out. The sensor can also output a 12-bit temperature and the altitude is a 20-bit measurement. This sensor will provide data about how high up we are above ground while flying with the drone.

### 3.3.3 Ultrasonic sensor

The ultrasonic sensor uses sound with 40 kHz frequency to send eight pulses of at least 10  $\mu$ s each and measures the time it takes for the sound to bounce on a surface and come back. Equation 4 is used to calculate the height in cm.

$$h = t * v / 100 / 2 \quad (4)$$

Where h is the height in cm, t is the elapsed time in seconds and v is the speed of sound at room temperature, 340 m/s. Division by 100 is to convert from meters to centimeters and division by two is because the elapsed time is both to and from the object it measures. The measurement range is between 2 cm to about 4.5 m and has a resolution of 0.3 cm. The angle it can measure is 15°. This sensor will be used close to the ground to measure the distance to an obstacle or the ground directly below the prototype.

## 3.4 Configuration and Filtering

The accelerometer can scale the measurement range from 2 g to 16 g. 2 g is double the free-falling acceleration and the range chosen for this project. The sample rate is 238 Hz and the anti-aliasing filter bandwidth is 50 Hz. The low pass filter cutoff frequency is the same rate divided by 50, which equals about 5 Hz. The measured pitch and roll angle is scaled down to 10 % and the previous angle is 90 % of the used angle fed to the control system to smooth out the movement of the prototype.

## **3.5 Software and development tools**

This section includes relevant software applications and integrated development environments used in a large portion of the project.

### **3.5.1 Telnet**

Telnet is a terminal emulation program that is used to access remote servers. Telnet is an acronym for Teletype Network and was developed in 1969. It is a bidirectional client-server protocol that uses port 23. The protocol collects data like attitude, height and converted user input from the WiFi-connected microcontroller on the prototype. Unfortunately, the protocol is old and unsafe because it sends plain text wireless, enabling anyone to listen to it. Because of this, it is not recommended to use in more sensitive systems where unauthorized user input is more dangerous. A safer protocol would be SSH, but Telnet is fast and easy for this setup.

### **3.5.2 Visual Studio Code and PlatformIO**

Visual Studio Code is a source-code editor created by Microsoft in 2015 for Windows, Linux and macOS. Features included in the program support debugging, syntax highlighting, code factoring and embedded Git. The editor can use various programming languages such as Java, Python, C++, Rust and more.[13]

PlatformIO is a cross-platform, cross-architecture integrated development environment for embedded system engineers. PlatformIO supports many software development kits(SDKs) and frameworks, debugging, unit testing, automated code analysis and remote management. In this project, it is used to code in the programming language C++ with the Arduino framework.[14]

### **3.5.3 Fusion 360**

Fusion 360 is a computer-aided design(CAD), computer-aided manufacturing(CAM), computer-aided engineering(CAE), and print circuit board(PCB) design software application available for Windows and macOS developed by Autodesk in 2013. This program is used to design and 3D print all the non-electric parts of the prototype.[15]

## 3.6 Implementation

This section describes in detail how the project is performed and designed with current parts in use, the layout of the component and how the automatic control system is implemented into the system.

### 3.6.1 Design and Construction

The tool's design is to be done in a CAD program called Fusion 360 with space for the continuous servos, microcontroller and other relevant hardware. The main design will then be manufactured in two pieces and the finished prototype will have one attachment point from each of the three servos to the drone[16]. This process is iterative to fix broken parts or add new features, such as the design of the gripper part. The system can resemble a tri-copter[17]. The hardware will be mounted on. The components will be soldered together and mounted to a breadboard. In the first phase, the main setup is done, including winches and the servos are controlled individually with the radio transceiver and one servo per channel, without Sbus implemented, and of course, research on how drones operate and control theory.

The two main non-electronic parts are designed and manufactured to assemble the first version of the prototype. The servos are attached with  $120^\circ$  rotation from each other on each corner of the triangle. See figure 7.

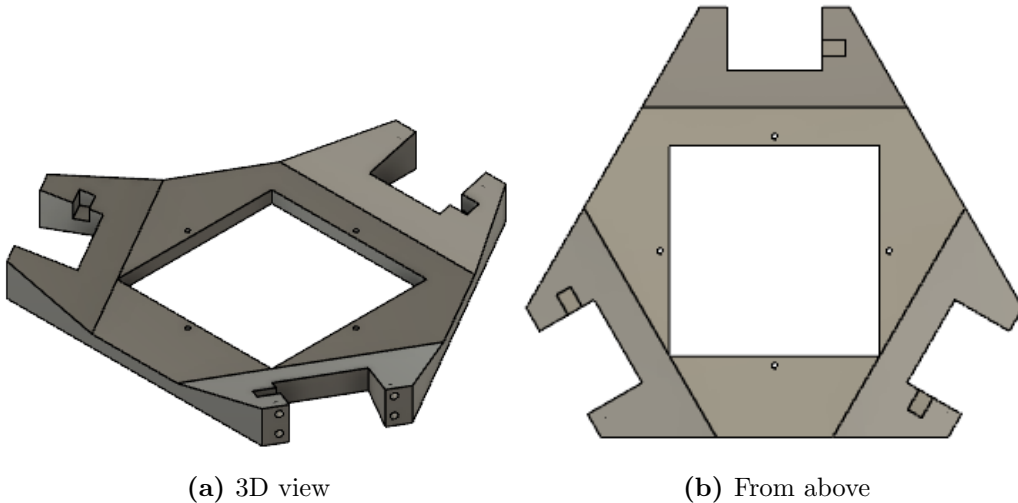


**Figure 7:** Triangle plate for servo and box

The box, seen in figure 8, is then placed in the hole in the center of the triangle plate from above and screwed down to keep it in place. The two pieces are separate because they are easier to produce and disassemble. The box has a special compartment for the battery to be strapped down and safe from harm. This phase also consists of deciding which electronics to use and a rough estimation of the power consumption for the whole system is done. Finally, this phase ended by testing the portable system with the battery as the power source.

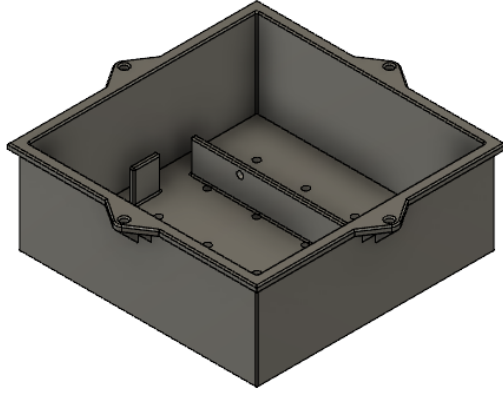


**Figure 8:** Box for electronics

### 3.6.2 Assembly and Configuration

Phase two mainly involves getting the prototype's stabilization to work and a user-controlled attitude in roll and pitch. This includes an automatic control system and implementation of SBus, PID-controller, mixer matrix, and IMU sensor to make them work together. We use filters to calibrate and minimize the disturbances and noise from the sensor samples before the controller processes them. A closed-loop feedback control system with a PID controller is developed to make the tool able to stabilize without manual user input[18] where the default set point values for the accelerometer of the  $x,y$ , and the  $z$ -axis is all zero. With user input, these change the set points accordingly. Here is also the prototype hung up for the time in three wires and this to work, a winch for each servo is made, which enables tests on the physical model. Tuning of the PID coefficients and some tests are made. The control system is further equipped with options to control the tool in 5 DOF manually. Over-the-air programming and Telnet communication are established to both

enable wireless updates of the software and also wireless serial monitor to collect data without external influence from a cable hanging down. The winches were made to endure the prototype pitching and rolling, which is why the design is in a cone formation. The 3D printed design is attached with four screws to the servo and the wire for each one is rolled up in the same direction where the counter-clockwise is up. The specific direction is made because the servos have a drift while on a standstill, biasing counter-clockwise. This means that if the wire is winded up counter-clockwise, being down, it will constantly be moving slowly downwards while powered on, which is not desired. However, counter-clockwise up makes the prototype's weight counteract the bias and is not moving while stable and powered on.

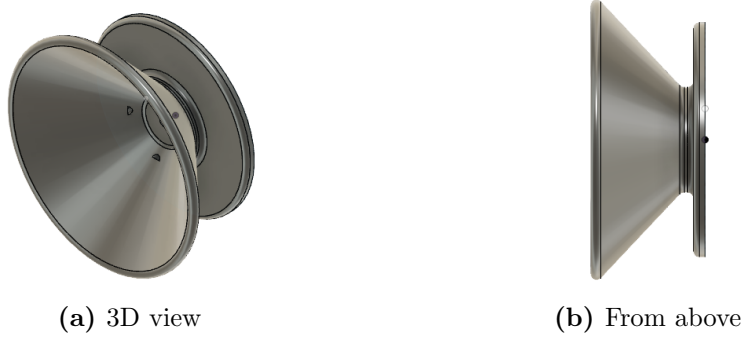


**Figure 9:** Winches for the servos

### 3.6.3 Anti-Swing and Optimization

The third phase of the project consists of implementing i) the gripper with the positional servo below the electronics box, ii) integrating the altimeter to measure the height from the ground, iii) the ultrasonic sensor to measure the distance to the closest surface or object below the prototype and iv) software development of a process to mitigate the impact of unwanted swing[3] and optimization of filters, hardware and configurations of the sensor and the code distribution.

The rest of the mechanical parts are also designed here. These are a case for the ultrasonic sensor, a mount for the gripper and wire holders. The case will have to expose the two cylindrical parts that transmit and receives the sound. The case is later attached under the electronics box pointing downwards.



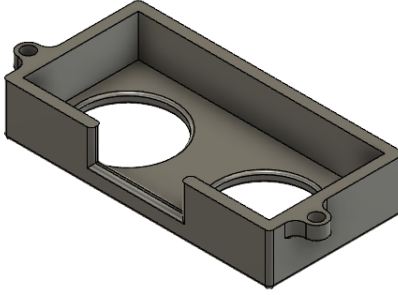


**Figure 10:** Case for ultrasonic sensor

The gripper was ordered as a complete product but without the servo and it can be seen in figure 11a but the objective is to grip a PET bottle and and, therefore, a mount to enfold the bottle is done for each arm and the design can be seen in figure 11b. Therefore, the two figures in figure 11 are not equally scaled.



(a) Standard model gripper[19]



(b) Bottle holder

**Figure 11:** Gripper to lift object with

The last non-electric part was what we could call a wire holder. It is attached with the upper screws on the servo to the servo plate. It is folded over the winch, which is previously mentioned to hold the wire so that it always comes in from the same angle and is placed relative to the winch, independent of the attitude of the prototype. The wire is going through the hole marked in red in figure 12. These were mounted on each winch the prevent the wire from falling off the winch and from controlling the placement of the wire in the winch.

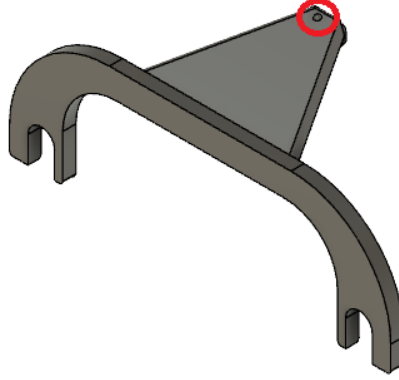


**Figure 12:** Wire holder for the winches with the wire hole red-marked

### 3.6.4 Mixer matrix

A mixer matrix is implemented to combine the values from the PID controllers and distribute the desired contribution to each servo motor. The matrix depends on how the sensor is oriented and becomes more accurate if the sensor has a fixed point relative to the prototype. Ideally, the IMU sensor has an x- and y-axis in the same direction as the prototype's pitch and roll. This is also assumed in this project after visual inspection and small tests. The last column corresponds to the elevation and has coefficients smaller than zero because, according to the sensor orientation, it is upside down on the setup. The elevation also does not have a magnitude of one like the other coefficients, which makes the elevation-move-down prioritized compared to pitch and roll movements. This enables those movements to be easier even if the prototype is simultaneously elevating. It is also dependent on the tuning of the controller.

$$\begin{bmatrix} ServoFront \\ ServoRight \\ ServoLeft \end{bmatrix} = \begin{bmatrix} Roll \\ Pitch \\ Elevation \end{bmatrix} * \begin{bmatrix} 0 & 1 & -0.8 \\ 1 & -1 & -0.8 \\ -1 & -1 & -0.8 \end{bmatrix} \quad (5)$$

### 3.6.5 Get attitude from x,y,z-components

The readouts from the acceleration sensor in the IMU are the acceleration in the x,y, and z-axis. These measurements are needed to calculate the roll and pitch angle. The definition of the expected acceleration data in these x,y,

and z-axis can be found in Equation 6[20]. When extracting  $\theta$  and  $\phi$ , which represent pitch and roll without the gravity component, we get the following relationship defined by its axis in equation 7 and 8.  $(\theta, \phi) \cdot \frac{180}{\pi}$  generates the pitch and roll angles in degrees.

$$a_m = \begin{pmatrix} g \sin \theta \\ -g \cos \theta \sin \phi \\ -g \cos \phi \sin \theta \end{pmatrix} \quad (6)$$

$$\theta_{accel} = \arctan\left(\frac{-a_x}{-a_z}\right) \quad (7)$$

$$\phi_{accel} = \arctan\left(\frac{a_y}{-a_z}\right) \quad (8)$$

The orientation of the x-axis is forward, the y-axis to the left and the z-axis is down. With these axis notations and equations 7 and 8, a positive pitch is with the front face downwards and a negative pitch is with the front facing upwards. Positive roll is equivalent to right sideways rotation and negative roll is left sideways rotation.

### 3.6.6 Attachment points to the drone

The attachment points will be in two sets to perform the tests with different conditions and see how much the test results differ. i) The attachment point is located close to where they are intended to be on the drone. The distance between the attachment point and the two behind is 125 cm and the measurement between the two in the back is 70 cm. The distance between the back two is less significant since the test will be done with a pitch movement. The prototype is symmetrical and should react in the same way as every angle and the usual way to operate a drone is mostly by movements forward and backward, which the tests will resemble. ii) The attachment points will be closer to each other, almost perpendicular to the ground. The distance from one wire to the other on the drone is 22 cm and the attachment points will be about 25 cm to be sure they are not too close to each other.

## 3.7 Process flow diagram of the PID controller

In this section, a part of the automatic control system is displayed as a process flow diagram to describe the method and implementation behind the system

visually. For example, in figure 13, we examine the process during a roll movement of the prototype. The process is restricted from rotating(rolling) with an angle of  $> 50^\circ$  in either direction to make the system more secure and have a margin of safety. The restriction is first visited in the desired state since the user can not demand a roll angle outside the approved limit. More on the restrictions later.

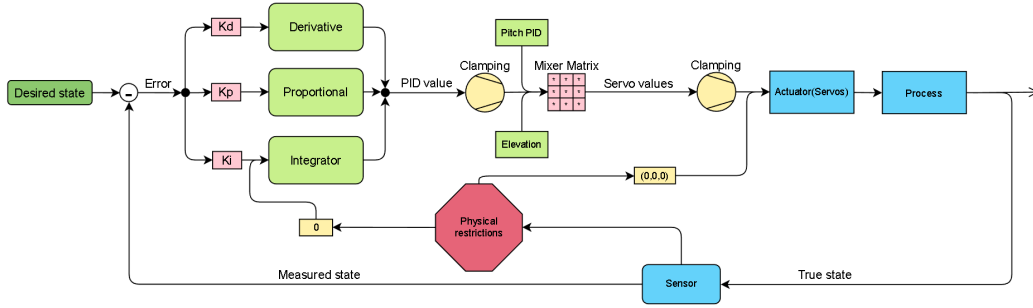


**Figure 13:** Automatic control system for roll

After the desired state is established, it is compared to the measured state from the IMU and the result is the error of the current iteration of the system. The error is then fed into the controller, which is a PID controller. The  $P$ -term is the target angle subtracted to the measured angle,  $I$ -term is the sum of all errors that is clamped to the servo limits. Lastly, the  $D$ -term is the error subtracted by the previous error. The terms are scaled in three ways with the constants  $K_P$ ,  $K_I$  and  $K_D$  corresponding to the controller's proportional, integrator and derivative part, which in simple terms, evaluates the influence from the present, past and future errors, respectively. These terms are added together to form the PID value. Here the restrictions are revisited in the form of clamping. The clamping checks if the result will correspond to the servo spinning full speed in one direction and the main reason for the clamping here is that one term should not grow big enough to make the other two insignificant. If the value exceeds the threshold value, the clamping will cut off the exceeded portion. Next in the system is the mixer matrix, where the pitch PID controller and the elevation are joined together in the matrix to output values for each servo individually. Before sending the desired speed to the actuators, the servos, in this case, another clamping, is made. Clamping is made in the same matter as the previous clamping process, but the main reason here is not to overexcite the servos.

Finally, the clamped desired speed vector is sent to the servos, which affects the physical model and rotates the prototype to reduce the error. The actual state is the exact angle of the model. The sensor calculates the angle and because of noise, the output is called the measured state since this state differs from the actual state. The measured state is compared to the desired state and another iteration of the process has begun. During the sensor block, a warning can be sent out if the measured state is not within the physical restrictions. The physical restriction is again  $50^\circ$  roll in either direction but also if the measured z-coordinate is below zero, which is, for example, if the prototype is upside down, more than  $90^\circ$  rolled or pitched in any direction or if it is falling faster than gravity towards the ground. When this happens, the integrator term is reset, and the servos are stopped independently of the PID values. This is implemented to minimize the risk of the prototype breaking itself or the drone it is attached to.

### 3.8 Hardware implementation

Similar to the previous section, a part of the project will be described visually with complementary text. In figure 14, a circuit diagram is displayed with all of the electric components included in the project. The core is the microcontroller ESP32 located in the middle of the figure and at the top left is the battery with the two step-down(Buck) converters which outputs 5 V and 6 V. The input of each electric component is labeled with an upwards-pointing triangle and the corresponding voltage. The ESP32 has much more pins, but only the important ones are present in this figure. Common ground is shared between all components and symbolizes a downwards-pointing triangle. On the left side of the microcontroller are two of the sensors, the IMU and the Barometer(Altimeter). They use 3.3 V input voltage and communicate through  $I^2C$ , which is also why they are connected to SDA and SCL.

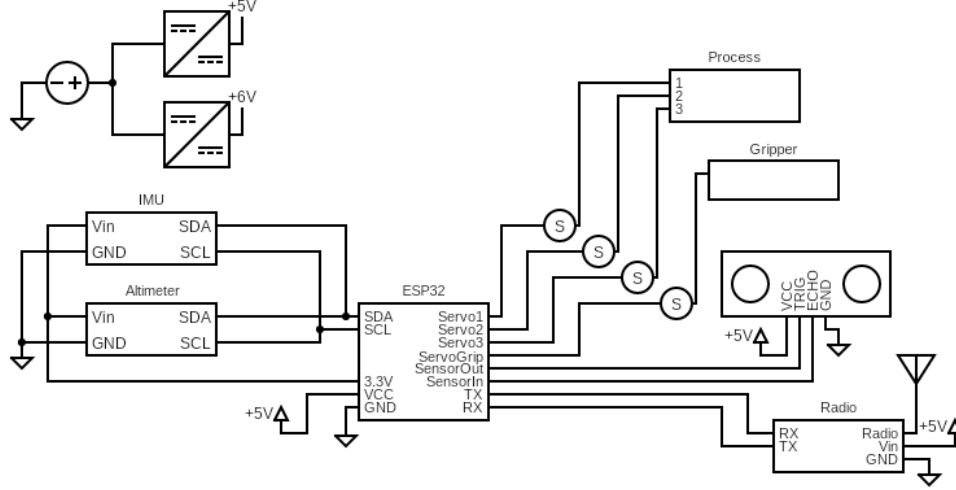


**Figure 14:** Circuit diagram with all components

On the bottom right side is the radio transceiver, the FrSky R10 Archer Pro, which uses 5 V input voltage from the battery via a buck converter, has a transmit/receive antenna to communicate through Sbus to the user controller and uses serial communication to communicate with the microcontroller. RX on the radio connects to TX on the microcontroller and vice versa. Just above the radio is the ultrasonic sensor. It is fed with a 5 V input voltage. This sensor sends and receives electrical impulses through two GPIO pins on the microcontroller. In the figure, the pins can be chosen arbitrarily and are called SensorOut and SensorIn. Last is the servos marked as a circle with an S. The first one from the bottom controls the gripper. The other three are used to control the winches and, by extension, the position of the full prototype, which was also previously called the process. All the servo has a 6 V input voltage. The servos are also connected to common ground.

### 3.9 Pinout

The section explicitly covers the microcontroller and how the pins are used for the other components. As we saw in the previous section, the microcontroller is powered by the battery through a buck converter to the pin called 5V0 and grounded through GND. GPIO0 and GPIO3 are typically used as TX

and RX, but those are reserved for serial communication through the wire if needed. Instead, the GPIO18 and GPIO19 are used as RX and TX pins to the radio. GPIO22 is the SCL, and GPIO21 is the SDA line. The pins GPIO32 and GPIO33 are used with the ultrasonic sensor as a sender trigger pin and receiver echo pin. GPIO26 is the output connected to the positional servo that controls the gripper. GPIO27, GPIO14 and GPIO12 output connected to the continuous winch servos. Finally, the pin labeled 3V3 is used to power the IMU and pressure sensor.

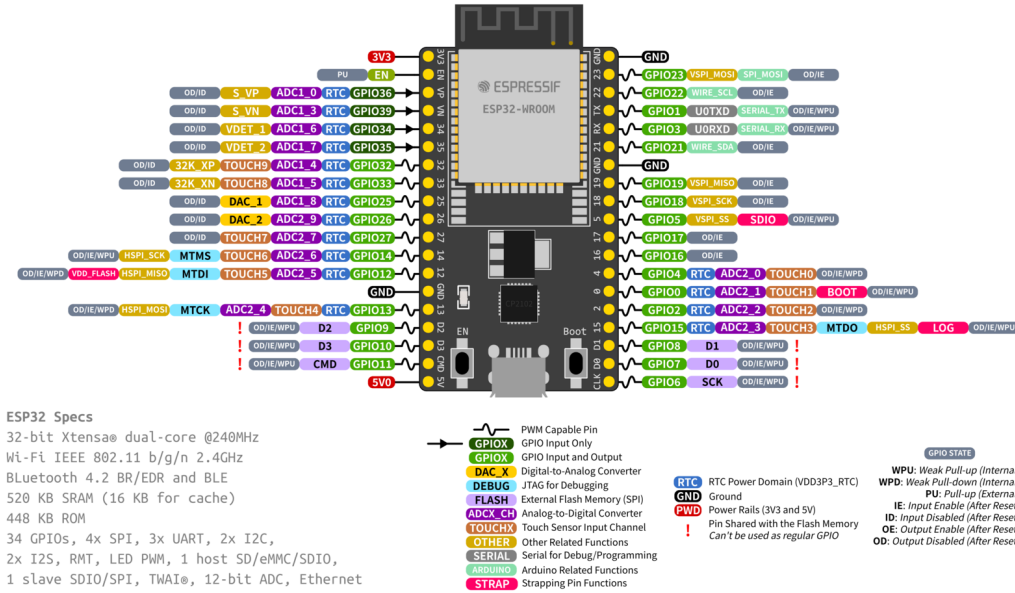


Figure 15: Espressif ESP32-DevKitC pinout[4]

## 3.10 Testing

Some tests are made to finalize the project and validate functionality compared to the goals and requirements. Those tests will be described in this section and conducted using the Telnet protocol for real-time sensor readouts.

### 3.10.1 Calibration

The calibration of the accelerometer measurement is tested. The initial calibration is made on a flat surface by computing the average offset of 100 samples, subtracting that offset from the actual samples and adding a one

on the z-component for gravity. The calibration can also be done during operation by clicking a button on the user control. What happens then is that the same process as the initial calibration starts and the servo is stopped.

### **3.10.2 Mobility and Functionality**

A test to see how the prototype responds to changing the desired roll and pitch angle. Test elevation up and down. Test mid-air calibration and test the gripper individually. The second test is to do everything at once, elevate down, pick up a load, move in 5 DOF with the load, elevate up and drop the load. This will be hard to document in this report but will be covered in the presentation.

### **3.10.3 Stability**

The stability is a center point in this project and will, of course, be tested. Stability is defined here when the prototype is parallel to the ground and stays there. This is tested in two ways. The first test is to power up the servos from an unwanted pitch and/or roll angle, minimize the error, and become parallel to the ground on its own, without external impact. The second test will start the process parallel to the ground and use the user controller to change the desired pitch and/or roll angle, with and without simultaneous elevation.

The same test will be made with another set of the attachment point, which is not realistic for the intended use of the prototype but will probably make it harder for the system to stabilize and thus gives more information about the system and area of use.

### **3.10.4 Anti-swing**

One of the more advanced goals was to prevent the prototype from uncontrolled swing, which resembled a gust of wind or a drone suddenly stopping after moving in a specific direction and the prototype continuing in the same direction, creating an unwanted swing. Three possible implementations of the two theories are invented starting with the first implementation. The change in elevation by lowering the body of mass in the center of the pendulum and raising it in the extreme positions. This implementation requires fast and unified servos with an accurate sensor software implementation for the system to know exactly when it should perform this. The system must



also perform passive leveling at the same time as the anti-swing implementation is active. This method is preferred on a pendulum using one wire. The second implementation covers the second theory about the swing set. Active target angling modification relies on the continuous change of the target angle variable to make the system stop swinging. Equation 9 is an example of how the system as a swing in the x-direction is initiated, where  $\alpha_{pitch}$  is the target angle, K is the scaling constant and  $a_x$  is the x-variable from the accelerometer. As the prototype is swinging this method will have the largest target angle offset and at position C in figure 4 it has the lowest offset. When the swing starts decelerating in position D and kinetic energy converts to positional, the  $a_x$  switches sign and the target pitch angle changes direction and starts pointing downwards. This method does also require fast servo and accurate sensor data processing and will be vulnerable to disturbance but can only be used with multiple wire and attachment points. Without an anti-swing implementation to a system like this but with perfect servos will then perform the passive leveling and because of that it will increase the swing.

$$\alpha_{pitch} = -K * \left(\frac{1}{a_x}\right) \quad (9)$$

The third implementation is active parameter reduction. The system has a PID controller with associated constants to control the passive leveling. Given that the prototype performs this task well you can decrease constants during the swing to make the system too slow to perform the task well and because of that follow behind the angle it should have and perform almost the same scenario as the second implementation. This does not require fast servos and must be used with multiple wires but will be more dependent on how far the attachments point are from each other. These three implementations assume that the system can indicate when the system is in a swing motion. How effective these implementations are probably highly dependent on the structure of the body as well as the position of the attachment points.

The third method is implemented in this project, mainly because of slow servos, and it is tested in two ways. First, the prototype will be dropped one meter from its neutral origin, with and without the winch servos powered on, to compare the outcome. Second, the prototype will be pushed from the neutral origin to approximately 300 cm, with and without servos powered on.

These tests will also be conducted with the second set of more narrow

attachment points. This will make the behavior of the prototype change to its original attachment point to stop the unwanted swing. Hopefully, the test with narrower attachment points enables the ratio between displacement and the pendulum's length.

### **3.10.5 Counteract yawing**

Test if the system can prevent the yaw rotation( $z$ -axis). This can be tested by letting go of the prototype, which is spun  $45^\circ$ . The same tests will be performed with the servos disabled. The IMU data will be observed during this test.

### **3.10.6 Attached to the drone**

Test how the prototype will act and react when attached to the drone. For example, it can still move in 5 DOF and perform the previous mobility and functionality tests. The main goal of this test is to answer the questions from the problem statement in section 1.2 that is:

“Is it possible to reduce disturbance, swing and errors by delegating some tasks to a subsystem on the tool to gain precision and dependability? How will such a tool affect drone movement and flight control?”

## 4 Results

This section presents the results from the performed tests of stability and functionality with both wide and narrow attachment points. In addition, the results of the design and construction will also be presented.

### 4.1 Design and Construction

The two main non-electronic components, the base plate and the electronics box, were made to carry the electronics in the smallest area possible with a structure that lasts and still has the center of mass reasonably close to the middle of the base plate triangle. The box has a square shape with a side of 8.4 cm and a height of 3.25 cm. The electronics can be soldered together and fit in the box, but components were placed on a breadboard for simplicity. The entire prototype weighs 613 g, including the breadboard. The final design has been working throughout the project with the battery safe in the battery compartment and nothing has been broken or replaced.

### 4.2 Tests

The following test figures showing the accelerometer's  $x$ ,  $y$ , and  $z$  parameters are presented in g's, which is  $9.82 \text{ m/s}^2$ . With this unit,  $z = 1$  is equivalent to the sensor being completely still concerning the ground, given that the sensor is perfectly parallel to the ground. The tests about mobility and anti-swing is also tested with attachment points approximately 30 cm to each other to perform the tests in other conditions. The attachment connected to the front servo was then tied to a rope to keep it in place.

#### 4.2.1 Passive leveling

A test were made to examine the stability and the result of the test can be seen in figure 16 where the system tries to keep a horizontal level. The function of detaching the servos through software is disabled during the testing. The prototype started horizontally and was not influenced by any noticeable external forces or disturbances during the test. The roll and pitch angle average is  $-0.8^\circ$  and  $0.4^\circ$  and has a standard deviation of  $0.75^\circ$  and  $0.49^\circ$ .

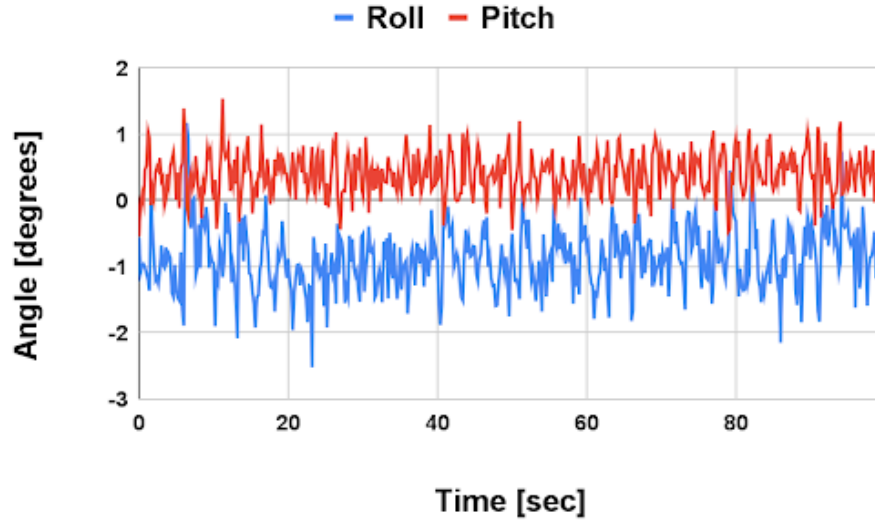


**Figure 16:** Stability test from horizontal without external influence

#### 4.2.2 Elevation

The two parts of mobility tested are the ability to control the altitude and the other is control attitude of the prototype, which is covered in the following section. The elevation is tested and measured with a sensor underneath the prototype. The measurement can not go to zero since the gripper is attached below the prototype and reaches further down than the sensor if self. This can be modified with an offset, but it depends on where it is desired to define the system's height.

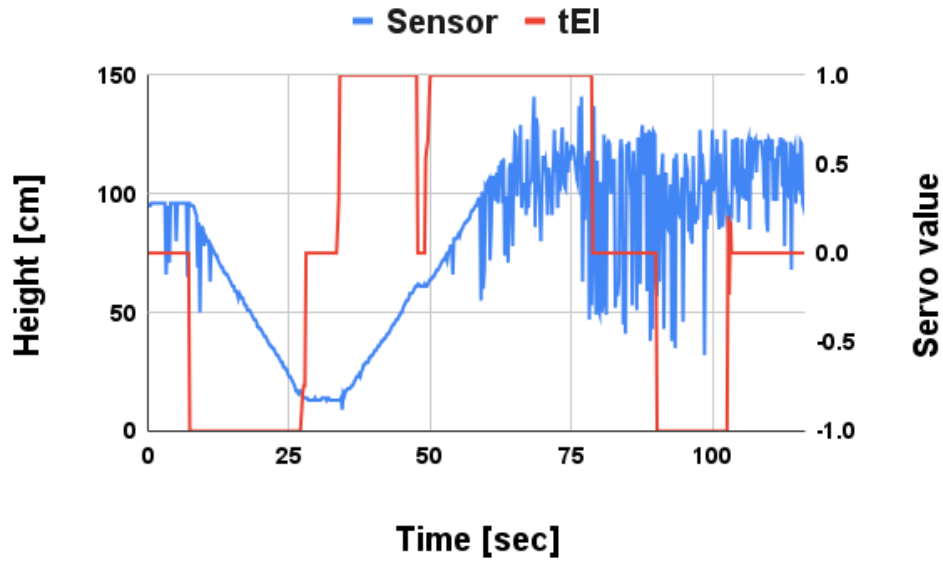


**Figure 17:** Height test with target elevation and distance to ground

In figure 17, tEI is the target elevation in servo speed where  $\pm 1$  is full speed from the user controller that is directly sent to the servo via the mixer matrix without a feedback loop. In red, named sensor, is the height measured with the ultrasonic sensor and tracked on the left vertical axis. The test started at the height of about 95 cm, followed by a full acceleration down and a quick stop before moving upwards again.

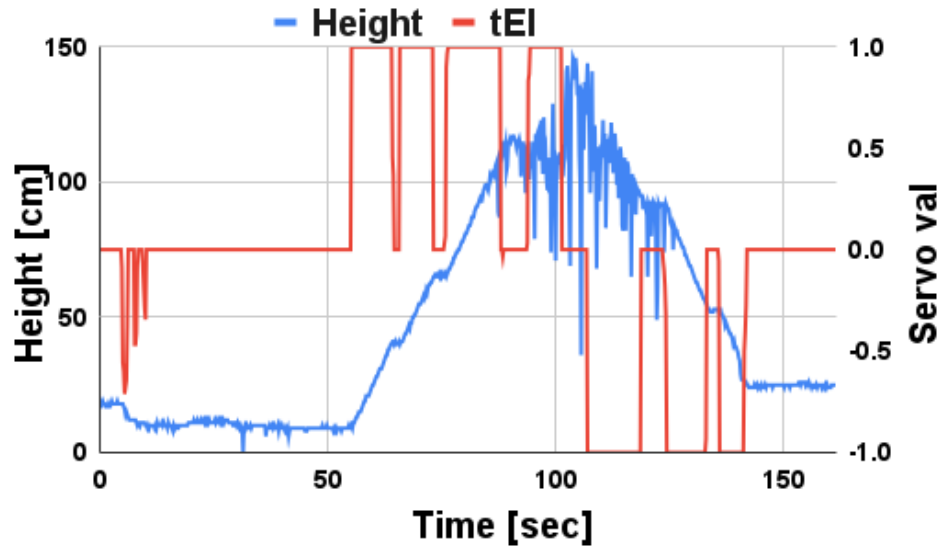


**Figure 18:** Elevation test with narrow attachment

The change in height test was remade with narrow attachment points in figure 26. The test starts with small movements downwards, followed by standing still, then an upwards elevation and ends with a downwards elevation. The graph shows in the same way how it can not provide accurate measurements above 100 cm but recovers fully after it reaches about 80 cm and continues to provide accurate measurements.

### 4.2.3 Mobility

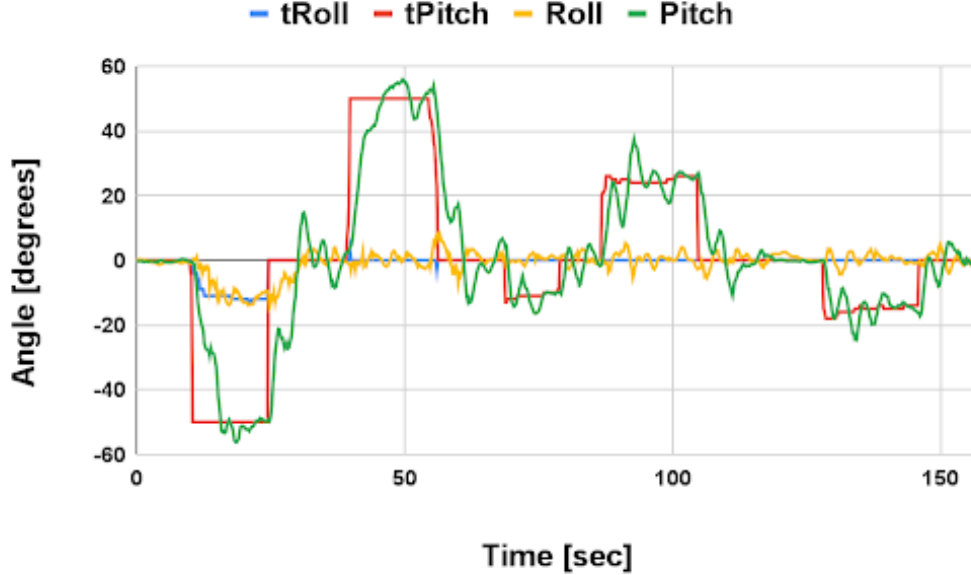


**Figure 19:** Target angles(tRoll, tPitch) and measured roll and pitch

In figure 19, the target angles is user-controlled. The test starts at a horizontal level followed by a small target roll of about  $10^\circ$  together with  $-50^\circ$  desired pitch. Then the desired pitch angle is changed a couple of times in both directions to capture behavior. The changes in the desired angles create an overshoot and oscillations. Since the attachment points are further from each other than the servo are on the prototype, a change in pitch results in rotation around the y-axis and but also movement in the x-direction as the front servo wire becomes shorter and the back servos becomes longer, which will affect the measurements while only looking at angles. Since the change in angle also induce a force in x-direction and moves the prototype, it will also move the the prototype forward(for this example) and when the target angle is reached the prototype will, because of the induced horizontal force, continue forwards a short distance. That short distance will result in overshoot and the swing that occurs will also result in oscillations.

#### 4.2.4 Functionality

The functionality is defined as the ability to utilize mobility in combination with the gripper and the sensor to perform simple tasks.

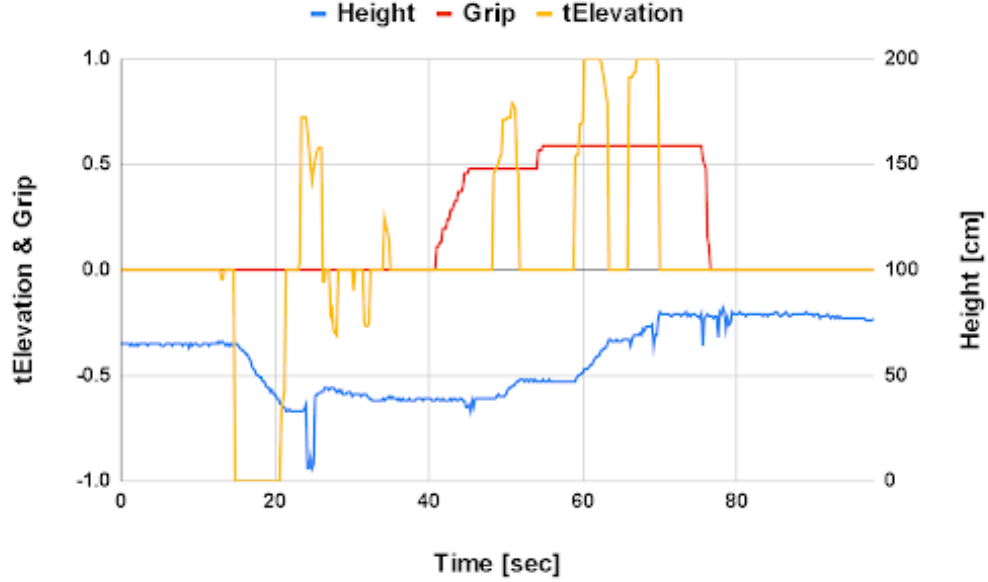


**Figure 20:** Grip and elevation test

The test with elevation changes in figure 20 includes the gripper and a PET bottle weighing about 1.5 kg. The left vertical axis tracks the target elevation and the grip. Zero in grip signify fully open gripper and one signify fully closed. It starts with the prototype being lowered towards the bottle on the floor. After some minor elevation changes to be able to grip the bottle, the gripper is closed and the bottle is lifted. The test ends with dropping the bottle while in the air. The other mobility test concentrates on the prototype's attitude in terms of roll and pitch according to the target angle of those measurements.

The test conducted in figure 21 tracks tElevation and Height parameters on the left vertical axis and the right tracks roll and pitch. The test started with a pitch angle of approximately  $40^\circ$  before the servos were powered on at about 12 seconds and it had the chance to stabilize. Then the prototype was elevated up and down to test the stability during operation the system does



experience and increasing roll angle during elevation as can be seen in yellow in figure 21 which can be explained by looking at the servo value during the same time interval. Figure 22 shows how the servos were operating during the same test. Y-axis represents the servo value where -1 and 1 correspond to full speed clockwise and counterclockwise, respectively. The servos generally follow a desired path, but singles instances give false values that make it jump to -1, 0 or 1, which affects the system's attitude, probably due to a software bug in the restriction function.

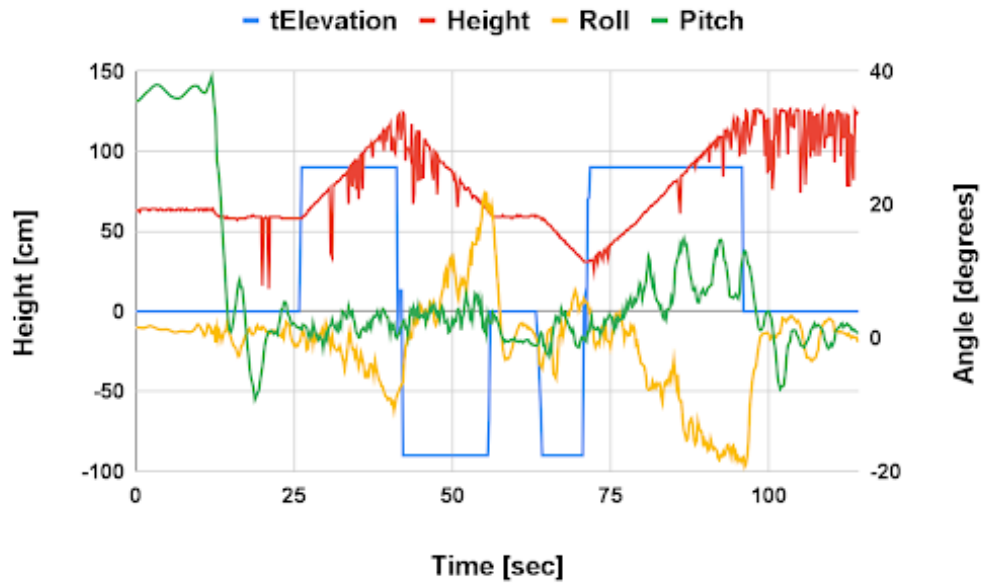


**Figure 21:** Stability from non-horizontal and during elevated

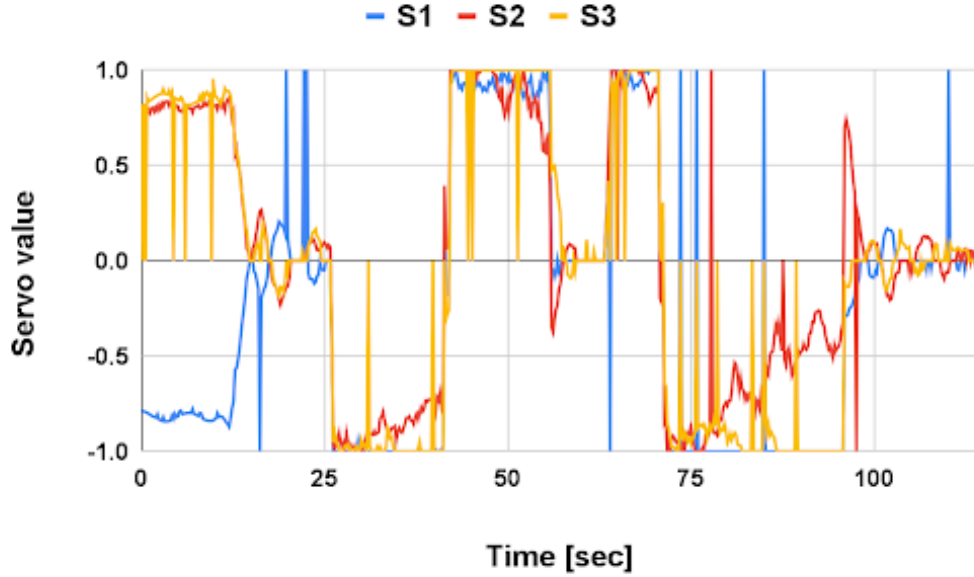


**Figure 22:** Servos during non-horizontal stability test

The mobility and functionality was tested together in figure 23 with the narrow attachment points for a complete view of how the system reacts. The right vertical axis tracks tElevation where 1 and -1 is fully up and fully down, respectively. The test start with pitch, a roll then a elevation up and down. Once again a undesired roll angle is present. Overshoot and oscillations are also present but smaller than with the wider attachment points.

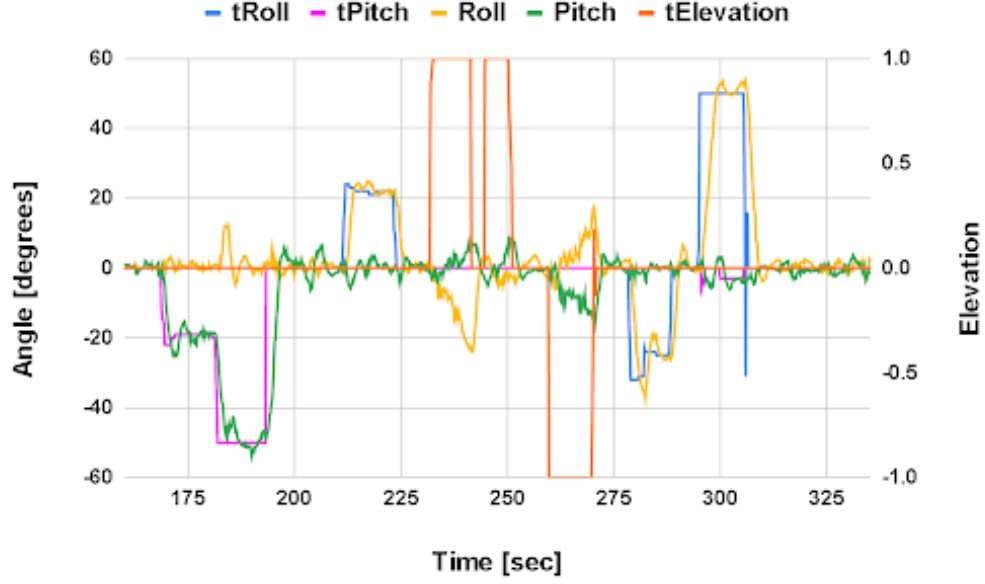


**Figure 23:** Functionality test of roll, pitch & elevation with narrow attachment

#### 4.2.5 Anti-swing

The test in figure 24 was without the servos powered on and the prototype was dropped 30 cm in negative x-direction from its resting position. After the drop, the system was not affected by any external forces or disturbances. The horizontal axis is time in seconds and the vertical axis is in g's.  $x$ ,  $y$ , and  $z$  is readings from the accelerometer.

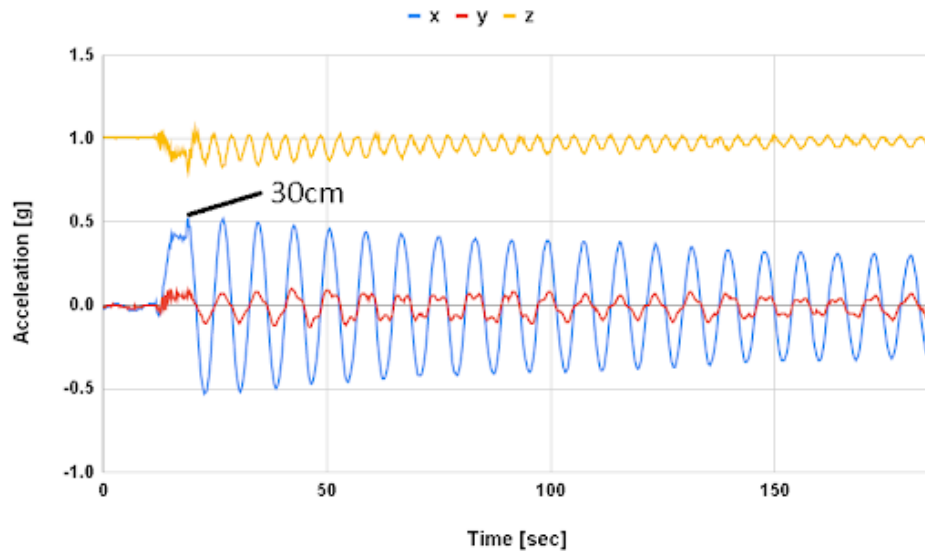


**Figure 24:** Swing without servos

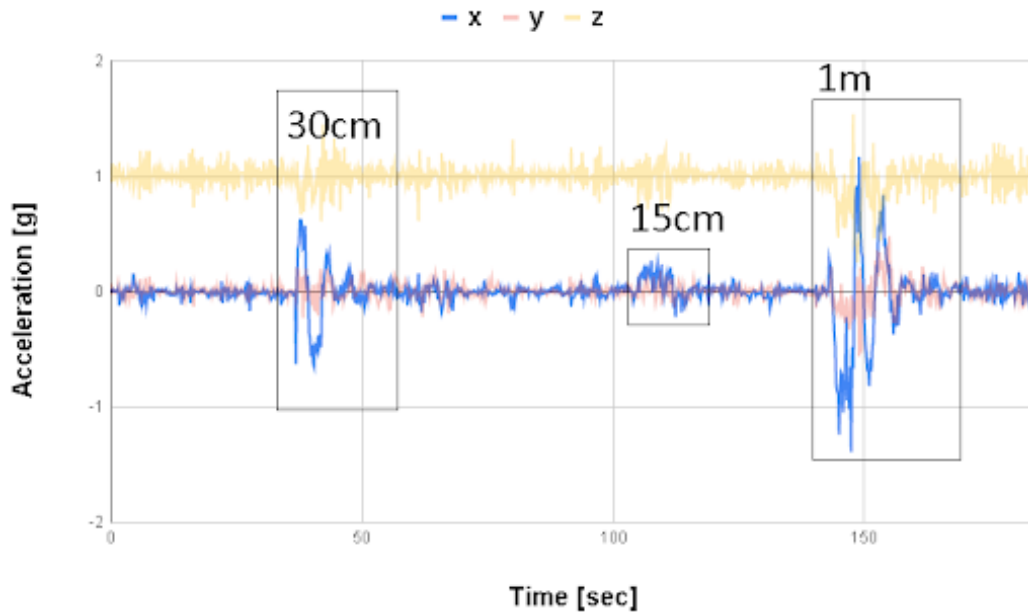


**Figure 25:** Anti-swing with servos and three external forces applied

Figure 25 displays the test about anti-swing with servos ON. The horizontal axis shows time and the vertical shows g's. The opacity of  $y$  and  $z$

readings are at 30 % to highlight the effect on  $x$  made by the external forces. The three external forces applied to the system are marked in figure 25. All the forces, in the form of pushes, tried to be only in the  $x$  direction to simplify the results. The first marked incident is a push that resulted in about 30 cm displacement. The second push is smaller than the previous, with about 15 cm displacement in the same direction. The last incident marked is a drop from 1 m displacement from the resting position.

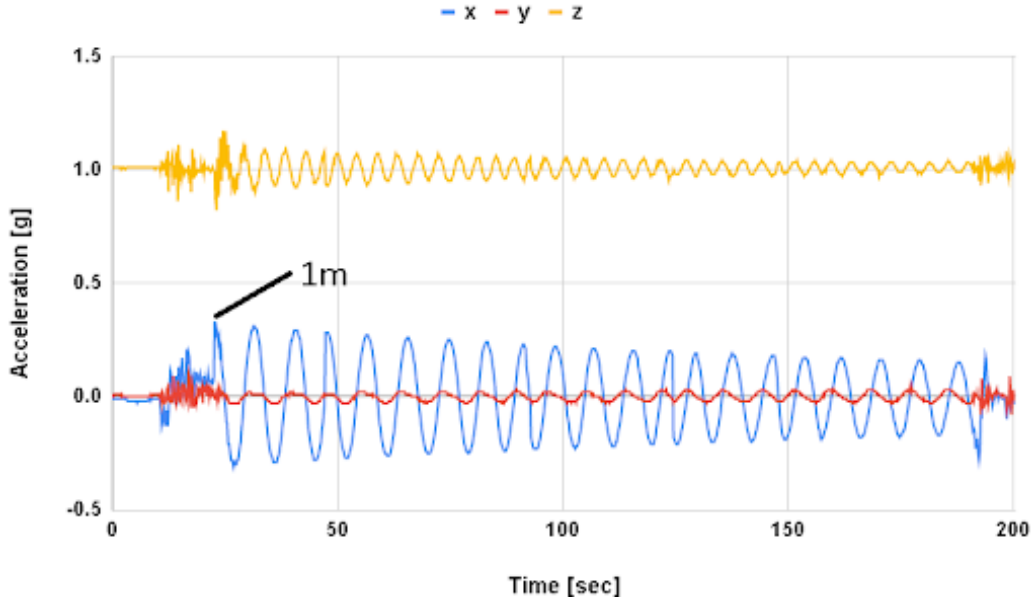


**Figure 26:** Swing with servos powered off from 1m

Same as before, a test is made to see the swing of the prototype without the servo powered on to provide a reference for when the servos are powered ON. The swing starts from 1  $m$  displacement to its resting position and is dropped with the intent that it should only move in the  $x$ -direction. We can also observe how smooth and continuous the acceleration in  $x$ -direction looks.

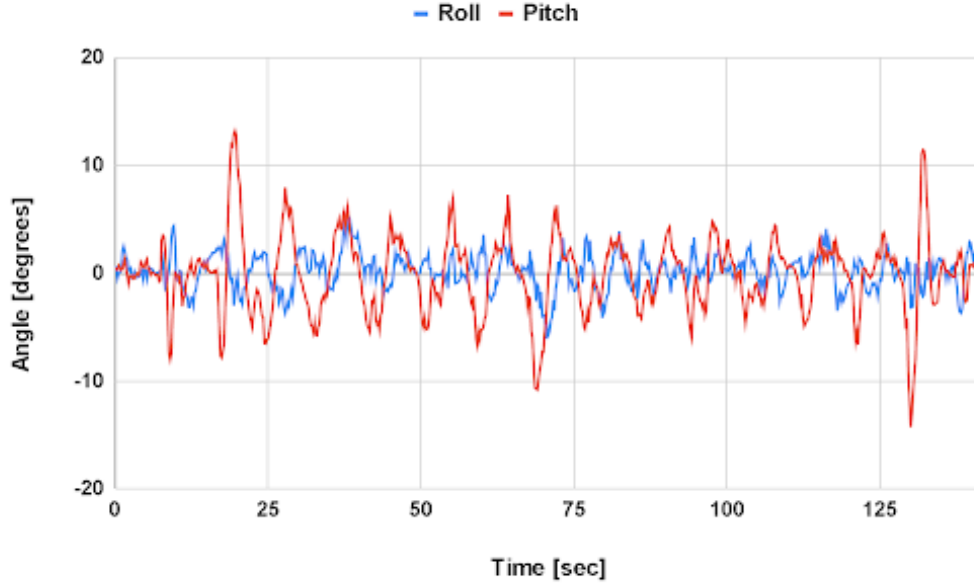


**Figure 27:** Roll and pitch during anti-swing

The same code used for the previous anti-swing test was still used and tested with the new attachment points. The graph in figure 27 shows roll and pitch with degrees on the vertical axis and time on the horizontal axis. The prototype was dropped the same way as before, but now with the servos powered on. The influence from the servos made the prototype start to yaw a little, which affected measurement. In figures 28 and 29, two graphs from the same test session as figure 27 show the values fed to the servos during the test and the accelerometer measurement in  $x, y, z$ .

A method to prevent yaw was not actively implemented and the system did not react differently with the servos ON compared to the servos OFF. Because of that, the results from the yaw tests is not included due to its insignificance.

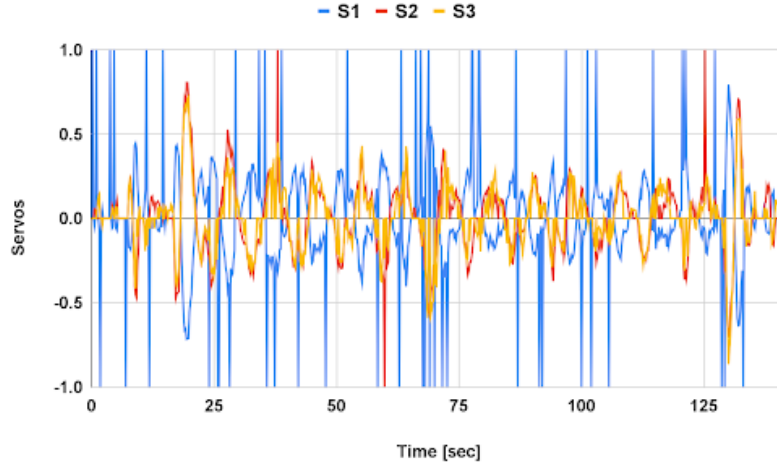


**Figure 28:** Servo writes during anti-swing

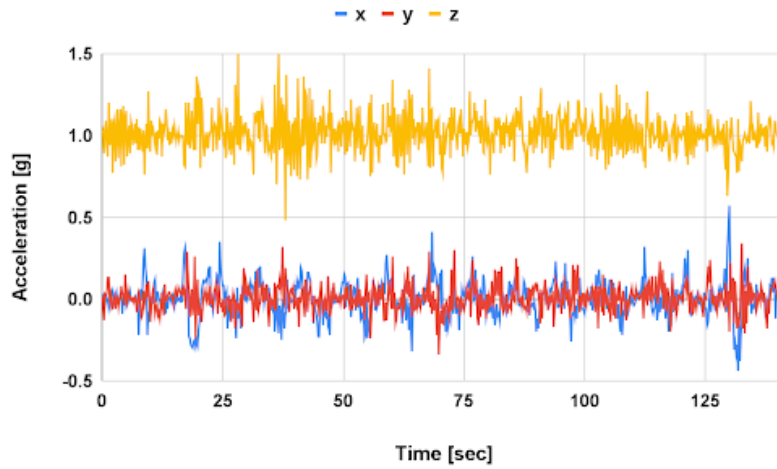


**Figure 29:** Accelerometer during anti-swing

#### 4.2.6 Accelerometer testing

Some of the tests contained a yaw movement of the prototype. Because of that, tests were made only with the accelerometer, first at a complete stand-still in figure 30 and then with rotation around the z-axis, with minimal

movements in the remaining 5 DOF that can be seen in figure 31. As mentioned before, the accelerometer measure movement in the directions  $x,y,z$ . Theoretically, this means that both graphs should be closely similar, but they are not, implying that the sensor is sensitive toward rotational movements.



**Figure 30:** Accelerometer at stand still

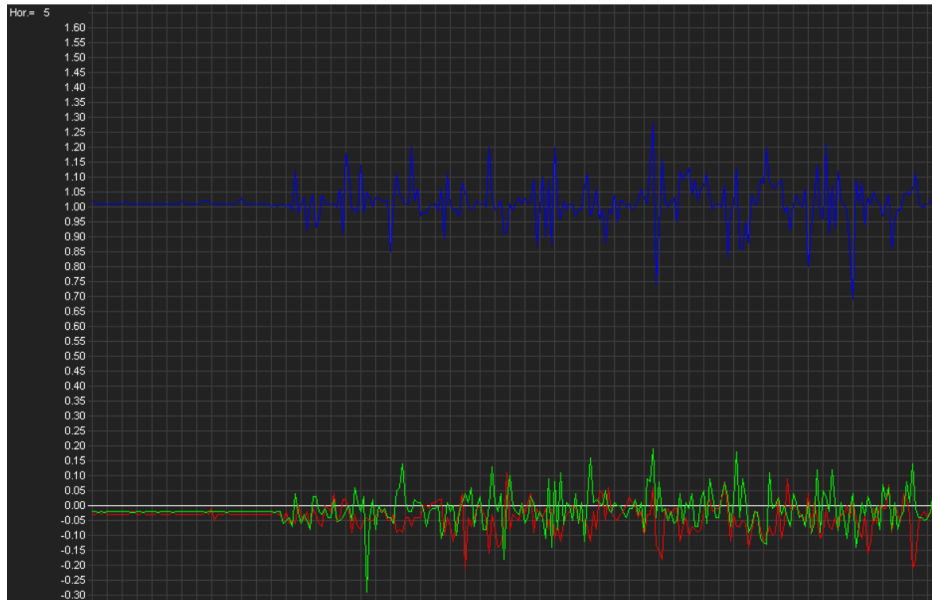


**Figure 31:** Rotational movement around the z-axis



#### **4.2.7 Attachment to the drone**

The drone team decided they could not attach the prototype to the drone due to lack of time which prevented the student from making some of the tests intended while attached to the drone and, to an extent, made the student unable to complete the last goal of the project.

## 5 Discussion and further work

In this section, the results will mainly be discussed with what went unexpectedly, why that was and suggestions for further work to continue with the project.

### 5.1 Analysis of the method

Overall the different connections between the hardware and user worked successfully with  $I^2C$ , SBus, OTA com. and Telnet. The current consumption was only monitored closer to the initial estimation upon the purchase since the optimal time of use is of high value, especially while adding more features and hardware. All the components except the battery were connected to the breadboard, which was strapped down on the prototype. The breadboard adds weight and cannot guarantee that the movement the IMU sensor experiences does not exceed the movements of the whole system and does not have unwanted vibrations. The better option would be to screw the IMU to the triangle plate to keep it steady relative to the actual motion of the system and to solder everything directly to their intended pin without the breadboard, which decreases wire use, resistance and, in some sense, weight. The 3D printed parts were not further stress tested to see their durability and were more on a "good enough to work"-basis. The servos were an excellent start for the first iteration of this model. However, they ended up being too slow, which can be transferred to the winches and making the wire drum wider and the movement appears faster, but it will also increase the torque, which was not observed during this project. The altimeter ended up not being used since the sensor's objective was to accurately measure the distance from the ground when the ultrasonic sensor was unable to. However, since the prototype was not connected to the intended drone, it never experienced those magnitudes of height and was excluded from the testing phase. The prototype could have been attached to something more robust and stiff together with a stiffer wire instead of a fishing line that was slightly too elastic, especially during added weight. The microcontroller has many more GPIO pins the take advantage of and the Telnet communication was fast and reliable with a WiFi connection.

## 5.2 Analysis of the results

As displayed in figure 17, 18 and 20, distances below about 100 cm can be accurately measured and the system responds fast to the user-controlled variables. The exciting part comes above 100 cm, where the measurement is no longer accurate and appears noisy. The high-frequency sound echoes from the ultrasonic sensor reflect on everything, which can explain the noisy appearance, but it is most likely because of how often the signal is sent. The distance is being measured at such a high rate that the signal from the first period can be observed by the second period, which will result in an inaccurately low distance measurement reading and continue to do so until the sensor comes close enough to a surface to send and receive the signal in the same period. The interval between each echo pulse can be increased but was not further improved due to prioritization. We can also observe how the sensor measures the distance to the PET bottle before closing the grip in figure 20 where the measured distance drops to about 6 cm and then continues to measure the distance to the floor again.

The stability of the system without external influence is examined in figure 16 within  $1^\circ$  and a standard deviation below  $1^\circ$ , which is within the definition of being stable for this project. With calibration and the servo detached, the mean and standard deviation can be even further improved. In figure 19, we can see the automatic control system's response and the reaction time as the target angle of either roll or pitch are changed. The measured roll and pitch successfully follow the user-controlled desired angles, noticeable in almost all the target angle changes followed by oscillations. The results also display the full range of mobility and even with a full forward or backward pitch of  $50^\circ$ , the system does not overshoot above  $60^\circ$ , which is below the physical restrictions of the system. As the prototype performs as a roll or pitch, it also moves sideways. With a small target roll or pitch, it is possible to keep it below  $5^\circ$  angle and control it in the x,y direction. Figure 21 starts from a nonparallel angle to the floor and once the servo gets powered on, the prototype goes too stable. As the target elevation is nonzero at various times, the roll angle does increase in magnitude. Since the user-controlled action is only elevation, this should not significantly affect the angle of roll and pitch. The servo values during this test displayed in figure 22 show the cause of the problem. A servo value below  $90^\circ$  does result in the servo moving upwards, values above  $90^\circ$  result in the servo moving downwards and on  $90^\circ$ , the servo should not be in movement. S1, S2 and S3 are the front, right

and left servos, respectively and we can see how the servo values at times jump from either 0 to 90, 90 to 180, or the opposite way and this is making the affected servo not leveled to the other two unaffected servos causing a roll without the ability to recover while the target elevation is nonzero. As the system stops experiencing user input, the system recovers and becomes stable, as shown on the right side in figure 21. The undesired servo values are most likely a software issue related to the physical restrictions given to the system.

### 5.2.1 Anti-swing

As the prototype is swung in the same direction for both in figure 24 and 25, the test can also be compared. With the servos powered off, we can observe a sinusoidal waveform with a slight linear decrease in amplitude. With the servos powered on, we can experience a much faster decay in the  $x$  variable, representing the swing in this test. Even with the drop from 1  $m$ , the system manages to be stable effectively. These are considered excellent results and valuable outcomes for the intended area of use. This is probably affected a lot by the placement of the attachment points and was further tested with the narrow points, which makes the wires almost entirely vertical and, in that way not be able to affect the horizontal movement directly and can only rely on the anti-swing theory previously mentioned which will be presented later in this section.

### 5.2.2 Test with narrow attachment

Figure 23 and 18 again show the functionality, mobility and response of the automatic control system, the rest of the software and the hardware. Elevation increases unintentional roll angle, and the ultrasonic sensor measurements do not reflect the actual distance in height from the ground but will recover as the prototype is lowered. The overshoot during a change in target roll or pitch angle is slightly less than with wider attachment points. This is probably because the change in attitude angle does not affect the horizontal movement in the  $x,y$  direction nearly as effectively as the compared test. However, when the target angle is changed using the wider attachment points, the prototype also moves in the  $x,y$ -plane, which provides a small unwanted swing that further extends the overshoot. This is not as significant with narrower attachment points, thus, about on average 60% lower

overshoot. It does, however, increase the presence of unwanted yaw since the wire is almost vertical and cannot be prevented solely by the tension force from the wires.

### 5.2.3 Narrow anti-swing

Since the wires are closer together, it affects a few things that we can observe in figure 26. First, the prototype can, without problem, be dropped from a 1 m displacement angle without servos ON. This is not possible with wider attachment points. Second, the x variable, which describes the directions of acceleration in the prototype is swung is a lot smaller even though the pendulum created moves wider. The tiny x values come from the prototype not performing as much of a pitch movement during the swing and therefore does not experience as much of the gravitational force.

To accurately compare the two anti-swing tests to each other, one should look at the same variables, which can be seen in figure 29. This, however, makes it challenging to figure out the movement of the prototype. It shows the rapid and unpredictable change in x,y- and especially in z-values as the z term is used to calculate both the pitch and roll angle. The anti-swing test results in figure 27 leave a more interpretative picture. It was not as good at counteracting unwanted swings and could not stay stable. This originates from three things. One is that the PID is not tuned for the lower changes in roll and pitch, which appear larger with wider attachment points. Two, the attachment point to the front servo is, as previously mentioned, tied to a rope from its original attachment point and this makes it much easier to affect than the other two attachment points, which partially explains why the measured pitch angle is in greater the measure roll angle during this test. The third is the servo and they occasionally get the wrong values of either 0 , 90 or 180 displayed in figure 28 and this further increases the change in pitch angle and the disturbance in the sensor values. The faulty values are probably caused by a software bug in the limitation methods. These together make preventing unwanted swings an impossible task for the current system and the current constants for the PID controller.

### 5.2.4 Accelerometer

Lastly, tests were made with the accelerometer to see how it reacts to yaw without filters, calibration and dampening factors. Since the accelerometer

measures the acceleration in x,y, and z, it should only be affected by those 3 DOF. First, the accelerometer output was observed while lying completely still on the table. The results of this test are shown in figure 30 and display three almost completely flat lines, which is expected by a non-moving sensor. The blue line is the z variable and it is close to zero because it experiences 1  $g$  acceleration towards the floor, which is the earth's gravitational force. In figure 31, the sensor rotates in a slow yaw movement. This movement should theoretically not affect the measurements at all. However, as we can see, it affects all three variables even though the sensor is detached from the prototype and can be assumed spin around its own z-axis. This is very good to keep in mind because all of the tests were made by hand. All the tests did experience some yaw movement, more with the narrower attachment point, which also explains the disturbance during testing. This can be seen with vibration. When the IMU sensor is attached to the prototype it is not exactly centered and will not spin around its z-axis and because of this further increase the disturbance. However, this disturbance, compared to the what is shown in 31 is insignificant.

## 6 Conclusion

This section will conclude if the requirements and goals are met. Overall, how well the project has been done and comments on possible improvements. This section will also review the problem statement and suggestions for future work.

### 6.1 Requirements

The prototype consists of a complete battery-driven system that can be attached to a drone with three winch-mounted servos that can be controlled wirelessly by a user and perform well for the intended distance between the attachment points. It can also pick up and drop a load controlled by the user. The weight, however, is not tested for the total 5 kg as required but instead with approximately 2 kg, which worked well. Furthermore, it was not tested because the fishing wires used were almost too elastic at the weight of 2 kg, which will affect the sensor and extent the automatic control system badly.

### 6.2 Goals

The system can effectively filter input data from the IMU sensor. The system can accurately estimate the current height and attitude in roll and pitch of the prototype. Furthermore, it can transmit valuable data wireless to the user during operation with the open network protocol Telnet.

The prototype will auto-stabilize without user-control with a control system for roll and pitch. It can also move in 5 DOF, including roll, pitch, elevation, forward and sideways, with the intended distance of the attachment points on the drone. This setup will also prevent unwanted swing, even though only one of the anti-swing implementations were tested due to slow servos. However, the prototype can not prevent or counteract yaw movement and has not been connected to the intended drone and flown outside.

### 6.3 Problem statement

With the results of this project, the student is convinced that it is possible to gain precision and dependability by delegating tasks like tool orientation and counteract unwanted sway. However, since the prototype was not tested with a drone, the student does not have results to back any statements about

the drone movement or the flight control other than that they will affect each other and inflict more disturbance and error on each system.

## **6.4 Further work**

The project has been an educational and enjoyable project with few initial restrictions and many possibilities and ways to work and develop as a working system which also makes the project easy to develop further and optimize.

### **6.4.1 Hardware & components**

The mechanical components designed for this project were made as proof of concept. They can be remade to increase durability, aerodynamics and rigidity. They had the sole function of working for the proof of concept and were not optimized for drone flight. These areas can be further researched and improved on those components. The power consumption of the electric components can be closely observed and an estimation of the time of operation per battery with current or extended functionality can be established. The choice and placement of components can also be optimized as the servo, for example, are too slow at the moment and the wire needs to be stiffer.

### **6.4.2 Software and the utilization of sensor data**

The software can be rewritten with label changes and object usage to make it easier to use and understand. The software restrictions on the system, such as clamping and angle limit, can be remade and more reliable. The sensor data can be filtered more and a secure network protocol can be used for data transmission to the user with, for example, SSH. The system can take advantage of the measurements from the gyroscope and magnetometer in the IMU with sensor fusion to mitigate the yaw disturbance in the accelerometer and get a more precise attitude measurement of the prototype. The constants used for the PID controller can be tuned with the help of fuzzy logic to maximize rise time and minimize overshoot and oscillations. Lastly, a method can be implemented to prevent unwanted yaw since it was not included in this report.



## References

- [1] S. Afzal, “What is I2C?.” <https://www.analog.com/en/technical-articles/i2c-primer-what-is-i2c-part-1.html>, 2020. [Online; accessed 29-November-2022].
- [2] Ashlin, “What is an automatic control system?.” <https://automationforum.co/what-is-an-automatic-control-system/>, 2021. [Online; accessed 21-November-2022].
- [3] T. Aldhizer, A. Morock, K. Hughes, M. Lanzerotti, S. Christoff, S. Lintelmann, and J. Capps, “Suspended load swing stabilization,” in *2020 IEEE Integrated STEM Education Conference (ISEC)*, pp. 1–6, IEEE, 2020.
- [4] “ESP32-DevKitC V4 Getting Started Guide.” <https://docs.espressif.com/projects/esp-idf/en/latest/esp32/hw-reference/esp32/get-started-devkitc.html>. [Online; accessed 30-September-2022].
- [5] G. Yakubu, P. Olejnik, and J. Awrejcewicz, “On the modeling and simulation of variable-length pendulum systems: A review,” *Archives of Computational Methods in Engineering*, pp. 1–19, 2022.
- [6] M. Pandolfo, “Modeling and control of a suspended load lifted by two aerial vehicles,” 2017.
- [7] M. Bisgaard, A. la Cour-Harbo, and J. D. Bendtsen, “Adaptive control system for autonomous helicopter slung load operations,” *Control Engineering Practice*, vol. 18, no. 7, pp. 800–811, 2010.
- [8] N. K. Gupta and A. Bryson Jr, “Automatic control of a helicopter with a hanging load,” tech. rep., 1973.
- [9] H. Emanuelsson and E. Sjunnesson, “Fjärrstyrt kamerafäste: He remote,” 2013.
- [10] “PID-regulator.” [https://en.wikipedia.org/wiki/PID\\_controller](https://en.wikipedia.org/wiki/PID_controller), 2022. [Online; accessed 22-November-2022].
- [11] A. Kavanaugh and T. Moe, “The pit and the pendulum,” *College of the Redwoods*, 2005.

- [12] “Specification of Product.” <https://www.gotronic.fr/pj2-fs5106r-2541.pdf>. [Online; accessed 01-December-2022].
- [13] “Visual Studio Code.” [https://en.wikipedia.org/wiki/Visual\\_Studio\\_Code](https://en.wikipedia.org/wiki/Visual_Studio_Code), 2022. [Online; accessed 30-November-2022].
- [14] “What is PlatformIO.” <https://docs.platformio.org/en/latest/what-is-platformio.html>, 2020. [Online; accessed 30-November-2022].
- [15] “Fusion 360.” [https://en.wikipedia.org/wiki/Fusion\\_360](https://en.wikipedia.org/wiki/Fusion_360), 2022. [Online; accessed 30-November-2022].
- [16] Ó. Pereira and P. Miguel, *Geometric Control of Thrust Propelled Systems*. PhD thesis, KTH Royal Institute of Technology, 2019.
- [17] N. M. A. Ahmed and M. H. Saleh, “Tri-copter drone modeling with pid control tuned by pso algorithm,” *Int. J. Comput. Appl*, vol. 181, no. 25, pp. 46–52, 2018.
- [18] T. Glad and L. Ljung, *Reglerteori: flervariabla och olinjära metoder*. Studentlitteratur, 2003.
- [19] “Standard gripper kit.” <https://www.electrokit.com/produkt/gripklo-for-standardservon/>. [Online; accessed 13-October-2022].
- [20] A. Kaviyarasu, “Fundamentals of attitude estimation,” 2020.

Appendix A: Gantt chart

